Supplementary materials

For

Tm-substituted 2:17-type Magnets: Balancing Room-Temperature Magnetic Properties and Temperature Stability

Table 1 Magnetic performance of $Tm_xSm_{1-x}TM_{7.6}$ magnets with different x. The H_k/H_{cj} is the squareness of demagnetization curves, Hci is the coercivity field at the demagnetization curves and H_k is the magnetic field corresponding to the magnetization of 90% of remanence at the demagnetization curves.

x	B_r (kGs)	H_{cj} (kOe)	$(BH)_{max}$ (MGOe)	H_k/H_{cj} (%)	$\alpha_{20\text{-}100℃}$ (%/℃)	$\alpha_{20\text{-}150℃}$ (%/℃)
0	9.82	42.26	22.61	90.44	-0.0541	-0.061
0.2	9.58	38.14	20.93	95.76	-0.0295	-0.0294
0.4	9.45	33.22	19.70	78.80	-0.0193	-0.0285
0.6	9.25	9.94	19.26	60.30	-0.0034	-0.0081
0.8	8.90	1.26	5.90	65.71	-	-
1	8.85	1.13	5.36	66.25	-	-

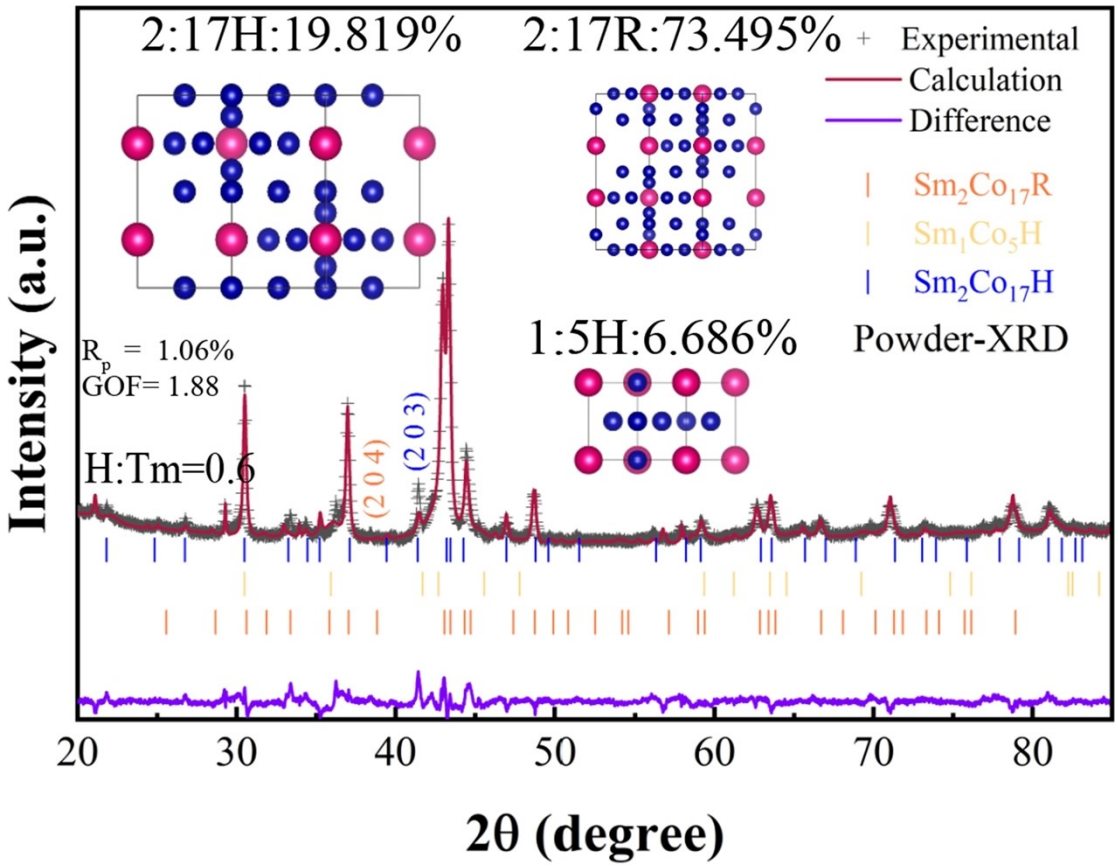

Figure S1 Rietveld refinement XRD patterns of HC-$Sm_{0.4}Tm_{0.6}TM_{7.6}$ magnets

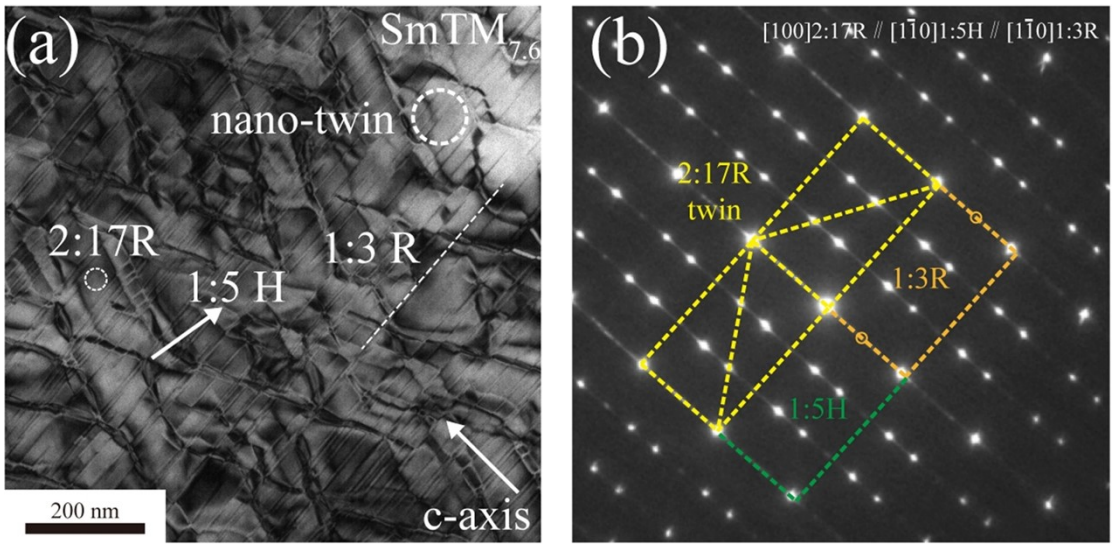

Figure S2 TEM bright-field image (a) and corresponding SAED pattern (b) of $SmTM_{7.6}$ magnets, respectively.

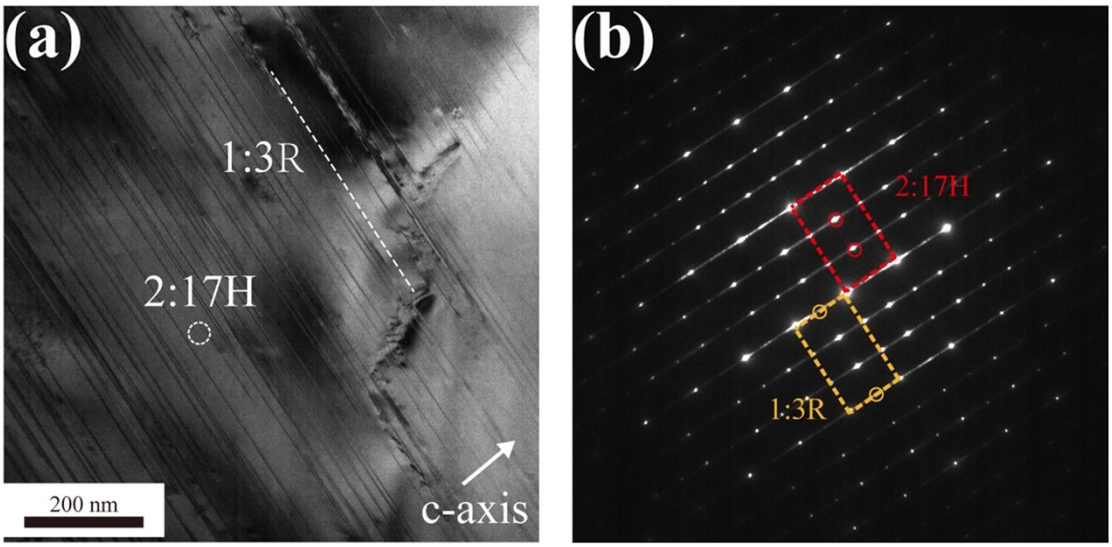

Figure S3 TEM bright-field image (a) and corresponding SAED pattern (b) of $TmTM_{7.6}$ magnets, respectively.

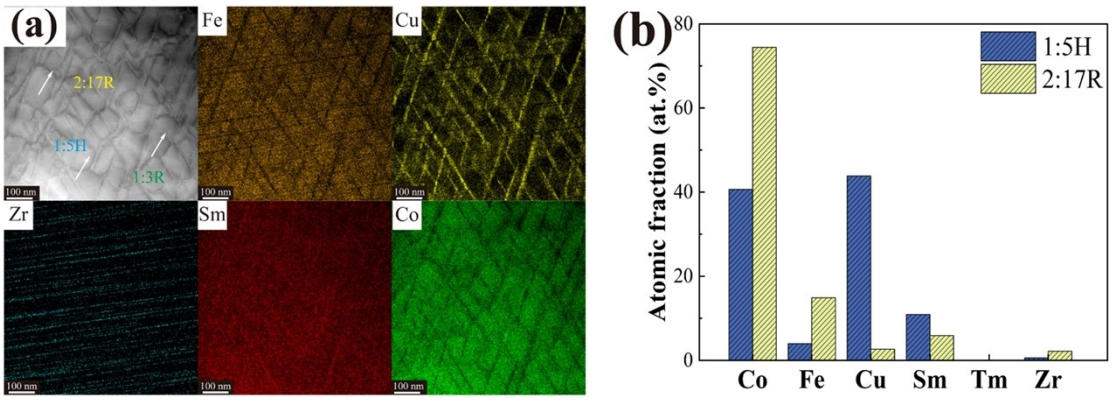

Figure S4 Elemental distribution in the cellular structures of $SmTM_{7.6}$ magnets. (a) HDAAF image and corresponding elemental distribution maps of Co, Fe, Cu, Zr, Sm, and Tm. (b) Point-scan results of the compositions of the cellular walls and intracellular phases.

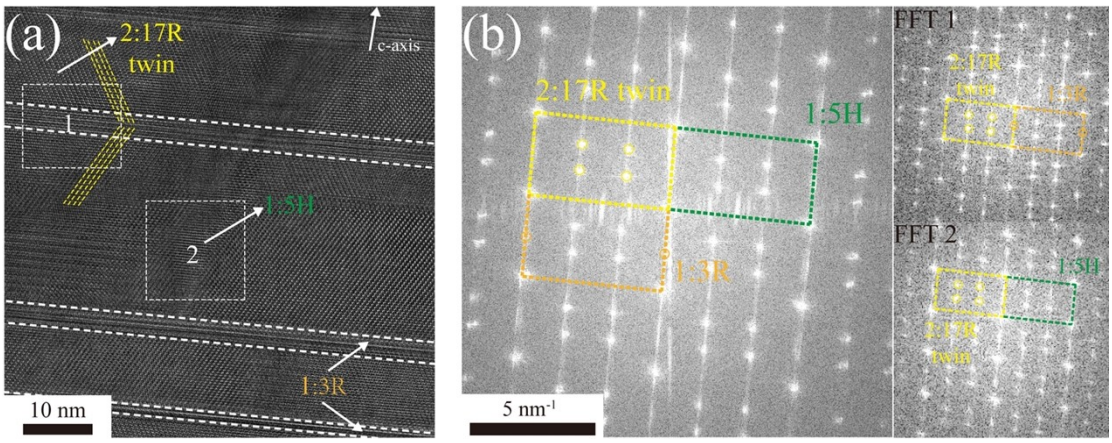

Figure S5 HRTEM image (a) and corresponding SAED patterns for $SmTM_{7.6}$ magnets.